Bioorganic & Medicinal Chemistry 18 (2010) 4702–4710

Contents lists available at ScienceDirect

Bioorganic & Medicinal Chemistry

journal homepage: www.elsevier.com/locate/bmc

Efficient RNA-targeting by the introduction of aromatic stacking in the duplex major groove via 5-(1-phenyl-1,2,3-triazol-4-yl)-2′-deoxyuridines

Nicolai Krog Andersen [a], Navneet Chandak [b], Lucie Brulíková [a,†], Pawan Kumar [b], Michael Dalager Jensen [a], Frank Jensen [c], Pawan K. Sharma [b,*], Poul Nielsen [a,*]

[a] Nucleic Acid Center,[‡] Department of Physics and Chemistry, University of Southern Denmark, 5230 Odense M, Denmark
[b] Department of Chemistry, Kurukshetra University, Kurukshetra 136 119, India
[c] Department of Chemistry, Aarhus University, Langelandsgade, 8000 Aarhus, Denmark

ARTICLE INFO

Article history:
Received 18 January 2010
Revised 5 May 2010
Accepted 6 May 2010
Available online 12 May 2010

Keywords:
Oligonucleotides
π–π-Stacking
Click chemistry
RNA-targeting

ABSTRACT

Three pyrimidine nucleosides with differently substituted phenyltriazoles attached to the 5-position were prepared by Cu(I)-assisted azide–alkyne cycloadditions (CuAAC) and incorporated into oligonucleotides. Efficient π–π-stacking between two or more phenyltriazoles in the major groove was found to increase the thermal stability of a DNA:RNA duplex significantly. The best stacking, and most stable duplex, was obtained by a sulfonamide substituted derivative.

1. Introduction

The nucleic acid duplex constitutes an excellent scaffold for chemically designed supramolecular chemistry.[1] The duplex is formed between complementary oligonucleotide sequences on the basis of selective hydrogen-bonding and strong π–π-stacking of the nucleobases. With the aim of targeting RNA-sequences by synthetic oligonucleotides, following the so-called antisense approach,[2] the idea of synthetically increasing the stability of the duplex by increasing the stacking has been approached in several ways including synthetic nucleobases with larger ring systems.[3] A major example is a tricyclic phenoxazine replacing a cytosine and increasing the thermal stability of a DNA:RNA duplex with up to 5 °C per modification.[4] Furthermore, the 5-position of pyrimidine nucleosides has been functionalised with the propyn-1-yl group[5] as well as with five-membered heterocycles,[6] and these modifications have been found to increase the duplex stability via increased π–π-stacking.

In our former study, we followed the concept of Click Chemistry[7] and studied the Cu(I)-catalysed azide–alkyne cycloadditions (CuAAC)[8] performed on 5-ethynyl-2′-deoxyuridine (**1**, Scheme 1).[9] This building block has been used for Click Chemistry conjugation of various moieties to DNA[10,11] and leads to the positioning of a triazole in the major groove of the duplex. We found that one triazole, either unsubstituted or substituted with a phenyl or a benzyl group, in general leads to decreased duplex stability, whereas four consecutive incorporations lead to significant duplex stabilisation of a DNA:RNA duplex.[9] Hence, a 9-mer duplex with four triazoles in the centre (replacing the 5-methyl groups of the bold thymidines in the duplex 5′-dGTG**TTTT**GC:3′-rCA-CAAAACG) displayed an increase in melting temperature of 14 °C as compared to the unmodified duplex, and a further 7 °C increase was obtained by phenyl substituted triazoles (**X** in Scheme 1). Modelling demonstrated (1) a clear preference for a coplanar orientation between the pyrimidine and the triazole with the C5 of the triazole oriented towards the O4 of the uracil (via a C–H···O interaction), and (2) a significant intrastrand π–π-stacking between the triazoles in the duplex involving to some degree also the phenyl groups. In combination with CD-spectroscopy, it was also shown that the duplexes are driven towards A- or A/B-type like duplexes by the introduction of the π–π-stacking triazoles.[9]

In the present study, we explore the scope of this stacking effect of phenyltriazoles concerning (1) the degree of modification in the duplex necessary to obtain the stabilisation, and (2) the effect of hydrophilic substituents in combination with electron-donating and withdrawing properties. We therefore decided to introduce a phenol and a sulfonamide (**Y** and **Z**, respectively, Scheme 1). To our best knowledge, this is at the same time the first introduction

‡ Nucleic Acid Center is funded by the Danish National Research Foundation for studies on nucleic acid chemical biology.

* Corresponding authors. Tel.: +45 6550 2565; fax: +45 6615 8780 (P.N.).
E-mail address: pon@ifk.sdu.dk (P. Nielsen).
† Present address: Department of Organic Chemistry, Faculty of Science, Palacký University, Tř. 17. Listopadu 1192/12, Olomouc 771 46, Czech Republic.

0968-0896/$ - see front matter © 2010 Elsevier Ltd. All rights reserved.
doi:10.1016/j.bmc.2010.05.019

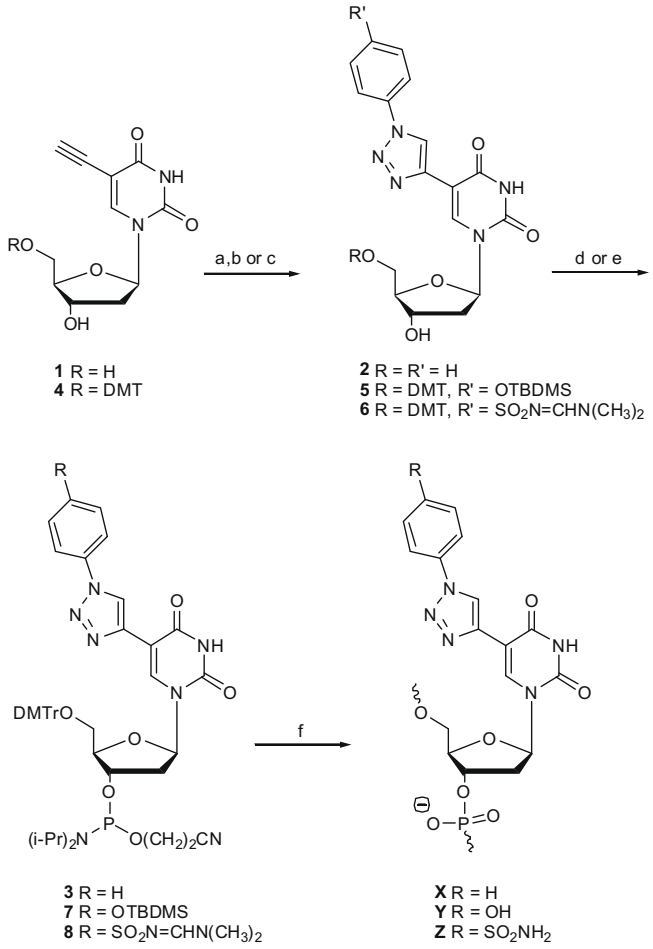

Scheme 1. Reagents: (a) Ref. 9: PhBr, NaN_3, CuI, Na ascorbate, EtOH, H_2O, MW, **2** 68%; (b) azide **10**, CuI, Na ascorbate, pyridine, EtOH, H_2O, **5** 78%; (c) azide **12**, $CuSO_4$, Na ascorbate, *t*-BuOH, H_2O, THF, pyridine, **6** 88%; (d) Ref. 9: (i) DMT–Cl, pyridine, CH_3CN; (ii) $NC(CH_2)_2OPClN(iPr)_2$, $EtN(iPr)_2$, CH_2Cl_2, **3** 42%; (e) $NC(CH_2)_2OPClN(iPr)_2$, $EtN(iPr)_2$, CH_2Cl_2, **7** 74%, **8** 67%; (f) automated DNA synthesis. DMT = 4,4′-dimethoxytrityl, TBDMS = *t*-butyldimethylsilyl.

of a sulfonamide into DNA. Ultimately, these aromatic nucleosides are extremely simple building blocks for the design of oligonucleotides with improved and selective hybridisation to complementary RNA and hereby an interesting potential in antisense therapeutics.[2]

2. Results and discussion

2.1. Chemical synthesis

In our first study, we prepared the triazole containing pyrimidine nucleosides directly from the unprotected 5-ethynyl-2′-deoxyuridine **1** using sodium azide, aryl or alkyl halides, and an in situ azidation/cycloaddition protocol (Scheme 1).[9] Each nucleoside, including **2**, was hereafter protected at the 5′-position by the 4,4′-dimethoxytrityl (DMT) group and converted to 3′-*O*-phosphoramidites in order to afford building blocks suitable for incorporation into oligonucleotides using standard automated solid phase DNA synthesis. By the phosphoramidite **3**, oligonucleotides containing the 5-(1-phenyl-1,2,3-triazol-4-yl)-2′-deoxyuridine moiety **X** were obtained.[9] For the present study, we obtained the best results by performing the cycloaddition reactions on the 5′-*O*-DMT-protected 5-ethynyl-2′-deoxyuridine **4** using azides that were prepared and isolated from suitable building blocks (Scheme 2). For introducing a phenol moiety, the protected azide **10** was prepared by direct silylation of the known *p*-azidophenol **9**, which has been prepared from *p*-bromophenol.[12] The TBDMS-group was chosen as an appropriately base-sensitive protection for the phenol group. For introducing a sulfonamide moiety, the known *p*-azidobenzensulfonamide **11**, made by a diazotation of *p*-aminobenzensulfonamide,[13] was protected with the equally base-sensitive dimethylamidine group to give **12**. The azides were reacted with **4** in the Cu(I)-catalysed cycloaddition to give the two protected triazole nucleosides **5** and **6** in good yields (Scheme 1). These were converted to the corresponding phophoramidites **7** and **8**, respectively.

The phosphoramidites **3**, **7** and **8** were successfully incorporated into oligodeoxynucleotides using automated solid phase synthesis with tetrazole as the activator and extended coupling times for the modified phosphoramidites. After completion of the synthesis, the oligonucleotides were removed from the solid support by treatment with concentrated aqueous ammonia. This treatment also removed all protecting groups including the silyl protection of the phenol and the amidine protection of the sulfonamide giving the incorporated monomers **Y** and **Z**, respectively, (Scheme 1). The three monomers **X**, **Y** and **Z** were incorporated into the same series of 9-mer oligonucleotides **ON1–ON6** (Tables 1 and 2). The constitution and purity of these were controlled by MALDI-MS and RP-HPLC, respectively.

2.2. Hybridisation studies

The series of oligonucleotides for this study was chosen with the purpose of finding the minimum of modification needed for duplex stabilisation. Hence, the 9-mer oligonucleotides with one and four incorporations of **X** in the centre, **ON1** and **ON6**, were taken from our former study,[9] whereas **ON2–ON5** represent different positions of a single modification as well as two or three consecutive incorporations of **X**. The same series **ON1–ON6** was hereafter prepared with both **Y** and **Z** (Table 1).

The hybridisation studies of the oligonucleotides were performed by UV-spectroscopy. For determining concentrations, extinction coefficients for oligonucleotides were determined by standard methods using extinction coefficients for the single nucleotides. For the modified monomers **X** and **Y**, the extinction coefficients at 260 nm for the deprotected phenyl[9] and hydroxyphenyltriazole nucleosides were determined by UV-measurements. Ab initio calculations of UV-spectra for a series of derivatives of **X** indicated no increased absorption at 260 nm for **Z** compared to **X** and therefore a similar extinction coefficient was assumed. In order to secure a concentration of 1.5 μM for the duplexes, however, a practical 50% lower coefficient for monomer **Z** was applied in the hybridisation experiments.

The oligonucleotides were mixed with the complementary DNA and RNA-sequences and the melting temperatures (T_m) of the resulting duplexes were determined. Table 1 shows the results

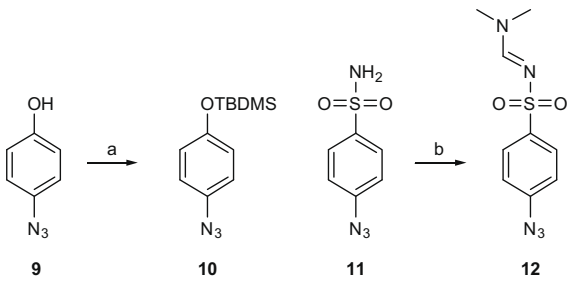

Scheme 2. Reagents: (a) TBDMS–Cl, DMAP, pyridine, CH_3CN, 90%; (b) DMF, $POCl_3$, 73%.

Table 1
Hybridisation data for DNA:DNA duplexes[a]

		T_m (ΔT_m/mod.)/(°C)[b]		
		B = X	**Y**	**Z**
ON1	5′-dGTG T**B**T TGC	28.0[c] (−5.0)	28.5 (−4.5)	28.0 (−5.0)
ON2	5′-dGTG **B**TT TGC	30.0 (−3.0)	29.5 (−3.5)	29.0 (−4.0)
ON3	5′-dGTG **BB**T TGC	30.0 (−1.5)	29.0 (−2.0)	31.5 (−0.8)
ON4	5′-dGTG T**BB** TGC	30.0 (−1.5)	28.5 (−2.3)	30.5 (−1.3)
ON5	5′-dGTG **BBB** TGC	30.0 (−1.0)	29.0 (−1.3)	33.0 (0.0)
ON6	5′-dGTG **BBB B**GC	32.0[c] (−0.3)	29.0 (−1.0)	35.5 (+0.7)

[a] Target sequence 5′-dGCA AAA CAC.
[b] Melting temperatures (T_m values/°C) obtained from the maxima of the first derivatives of the melting curves (A_{260} vs temperature) recorded in a medium salt buffer (Na_2HPO_4 (5 mM), NaCl (100 mM), EDTA (0.1 mM), pH 7.0) using 1.5 μM concentrations of each strand. In brackets the changes in melting temperature for each modification **B** (ΔT_m/mod./°C) as compared to the unmodified reference duplex (T_m = 33.0 °C).
[c] Data taken from Ref. 9.

Table 2
Hybridisation data for DNA:RNA duplexes[a]

		T_m (ΔT_m/mod.)/°C[b]		
		B = X	**Y**	**Z**
ON1	5′-dGTG T**B**T TGC	29.0[c] (−2.0)	30.5 (−0.5)	30.0 (−1.0)
ON2	5′-dGTG **B**TT TGC	30.0 (−1.0)	29.0 (−2.0)	29.0 (−2.0)
ON3	5′-dGTG **BB**T TGC	35.0 (+2.0)	37.0 (+3.0)	35.5 (+2.3)
ON4	5′-dGTG T**BB** TGC	37.5 (+3.3)	39.0 (+4.0)	39.0 (+4.0)
ON5	5′-dGTG **BBB** TGC	43.0 (+4.0)	45.0 (+4.7)	46.0 (+5.0)
ON6	5′-dGTG **BBB B**GC	51.5[c] (+5.1)	51.0 (+5.0)	55.5 (+6.1)
Mismatch sequences[d]				
ON6	5′-dGTG **BBB B**GC 3′-rCAC ACA ACG	24.0[c] (−27.5)	26.5 (−24.5)	nt[e]
ON6	5′-dGTG **BBB B**GC 3′-rCAC AGA ACG	42.0[c] (−9.5)	41.0 (−10.0)	46.0 (−9.5)
ON6	5′-dGTG **BBB B**GC 3′-rCAC AUA ACG	31.0[c] (−20.5)	29.0 (−22.0)	*nt*[e]

[a] Matched target sequence 5′-rGCA AAA CAC.
[b] Melting temperatures (T_m values/°C) obtained from the maxima of the first derivatives of the melting curves (A_{260} vs temperature) recorded in a medium salt buffer (Na_2HPO_4 (5 mM), NaCl (100 mM), EDTA (0.1 mM), pH 7.0) using 1.5 μM concentrations of each strand. In brackets the changes in melting temperature for each modification **B** (ΔT_m/mod./°C) as compared to the unmodified reference duplex (T_m = 31.0 °C).
[c] Data taken from Ref. 9.
[d] Mismatch studies, in brackets the changes in melting temperature as compared to the matched duplex **ON6**:RNA.
[e] No transition observed.

obtained with modified DNA:DNA duplexes. A single incorporation of either of the modified monomers **X**, **Y** or **Z** once in the centre of the duplex, **ON1**, lead to a significant decrease in duplex stability as validated by T_m's around 5 °C lower than for the unmodified duplex. The same was observed for **ON2** although the decreases in T_m were somewhat smaller. With the second incorporation of the modified monomers, in **ON3** and **ON4**, the relative destabilisation was even less pronounced, especially in the case of the sulfonamide **Z** (ΔT_m = −0.8 °C per mod.). The same trend continued with three incorporations, **ON5**, and with four modified nucleoside monomers, **ON6**, the decrease in duplex stability was fully compensated by the stacking of the modified nucleobases. Hence, the duplex stabilities were similar to the unmodified duplex, varying from a small decrease with the phenol **Y** (ΔT_m = −1.0 °C per mod.) to a small increase with the sulfonamide **Z** (ΔT_m = +0.7 °C per mod.).

Table 2 shows the hybridisation data of the modified DNA:RNA duplexes. A single incorporation of either **X**, **Y** or **Z**, in **ON1** or **ON2**, lead to decreases in thermal stability that were somewhat smaller than with DNA:DNA (ΔT_m's between −0.5 and −2.0 °C). This picture changed significantly by the introduction of the second modified nucleoside. **ON3** displayed significantly increased duplex stabilities, and in the slightly different sequence **ON4**, even further increases were observed with ΔT_m's up to +4 °C per modification. The tendency continued by three and four incorporations in **ON5** and **ON6** revealing further relative increases in duplex stability with ΔT_m's up to +6.1 °C per modification for the four sulfonamide substituted phenyltriazoles **Z**. Interestingly, the hyperchromicity observed for the melting of a duplex generally decreased by the numbers of monomer **Z** but not in the case of monomers **X** and **Y**. Nevertheless, the melting transitions were clearly determined.

Comparing the data for the modified DNA:RNA duplexes in a different way, the introduction of the second phenyltriazole moiety on the top of the first gave an increase in T_m of 5 °C (compare **ON3** with **ON2**, Table 2) or even 8.5 °C (compare **ON4** with **ON1**) for **X**. The third incorporation of **X** gave an increase in T_m of 5.5 or 8 °C (compare **ON5** with **ON3** or **ON4**), and the fourth incorporation of **X** gave a further increase in T_m of 8.5 °C (compare **ON6** with **ON5**). The corresponding increases in T_m for the phenol moiety **Y** were +8/8.5° for the second, +6/+8 °C for the third and +6 °C for the fourth incorporation. For the sulfonamide **Z**, the increases in T_m were +6.5/9° for the second, +7/+10.5 °C for the third and +9.5 °C for the fourth incorporation.

The remarkable RNA recognition was further investigated by mismatch studies. Hence, **ON6** with either **X**, **Y** or **Z** was mixed with RNA-sequences containing a single central mismatch, and the melting temperatures of the mismatched duplexes were determined (Table 2). In most cases, fine mismatch discrimination was observed as indicated by the large decreases in T_m relative to the matched duplexes formed by **ON6**. A to C mismatches were perfectly discriminated by **X** and **Y** (ΔT_m values of −27.5 and −24.5 °C, respectively), whereas no mismatched duplex by **Z** could be detected. Similar results were observed for the A to U mismatches, whereas the discrimination of the A to G mismatches was slightly smaller for all the three modifications **X**–**Z** (ΔT_m's around −10 °C). This is however similar to unmodified DNA:RNA duplexes, where the A to G mismatch is the most stable of the three.

The fact that two mismatched duplexes formed by **ON6**-**Z** were not detectable by UV-spectroscopy was puzzling but seemed associated with the generally low hyperchromicity observed for the DNA:RNA duplexes with **Z**. With the local denaturation induced in the middle of the duplex by a mismatch the transition might be undetectable by the UV-methodology.

2.3. Circular dichroism spectroscopy

To further study the influence of π–π-stacking and the stepwise increasing modification on the duplex structure, circular dichroism (CD) spectroscopy was applied. It is well known that DNA:DNA duplexes adopt a B-type form in solution, whereas RNA:RNA duplexes adopt an A-type and DNA:RNA duplexes intermediate A/B-type structures. A- and B-type duplexes are known to display distinctly different CD spectra. A-type duplexes give an intense negative band at ~210 nm and a positive band at ~260 nm, whereas B-type

duplexes give a negative band at ~250 nm and positive bands at ~220 and ~280 nm. For this study the unmodified DNA:DNA duplex was taken as a standard for the B-type, and the CD-spectrum (Fig. 1) clearly displayed the B-type characteristics. The DNA:RNA duplex showed the expected intermediate A/B-type with some clear A-type characteristics. The single incorporation of monomer **X** in **ON2** indicated that the DNA:DNA duplex retained its inherent B-type form (Fig. 1). This is similar to what was observed for **ON1-X** in our first study.[9] However, the double incorporation of **X** in **ON3** and **ON4** resulted in two slightly different CD-curves. **ON3** resembled **ON2**, whereas **ON4** showed a small shift of the band at 280 nm towards 275 nm. Upon the triple incorporation of **X** in **ON5** we observed a further small shift towards the A/B-type helical form with a beginning shoulder at 265 nm and a decreasing negative band at 250 nm. This is fully in accordance with our previous observations for **ON6-X**.[9]

For the DNA:RNA hybrid duplex, only small changes in the CD-spectra were observed by the introduction of **X** (Fig. 2). Hence, all curves were similar to the one obtained from the unmodified DNA:RNA duplex indicating that the modifications are not changing the overall A/B-type duplex structure. This is consistent with our first study where both **ON1-X** and **ON6-X** displayed similar CD-curves with RNA.[9]

In the case of the sulfonamide modification **Z**, the CD-curves revealed somewhat different observations. For the DNA:DNA duplex, the single modification in **ON1** demonstrated almost no changes in the CD-spectrum, whereas the spectrum for **ON2** demonstrated a lower band at 280 nm and a beginning shoulder at 265 nm (Fig. 3). With the two modifications in **ON3** and **ON4**, this trend continued with the largest changes observed for **ON3**. In other works, both the number of modifications and the sequence context influenced the gradual change in duplex structure. With the three modifications in **ON5**, an even larger band at 265 nm was seen indicating the expected shift towards an A/B-type duplex but also other changes in the CD curve were seen. With **ON6**, the positive band has moved backwards to 275 nm, and the negative band at 250 nm has become very small.

For the DNA:RNA duplexes containing the sulfonamide **Z**, all CD-spectra indicated that the modified duplexes had an A/B-type hybrid duplex conformation not differing significantly from the unmodified DNA:RNA duplex (Fig. 4). With the increasing number of modifications, however, the intensity of the negative band at 250 nm was decreasing and moving towards 235 nm, and a new small positive band appeared at 310 nm.

2.4. Molecular modelling

The DNA:RNA hybrid duplexes formed by the oligonucleotides with two and four consecutive incorporations of monomer **X**, **Y** and **Z** (**ON3** and **ON6**) were built in MACROMODEL[14] and studied in molecular dynamics simulations. The initial hybrid structures were built in the B-type duplex conformation and the incorporated monomers were subjected to a Monte Carlo conformational search verifying the C5 (pyrimidine)–C4 (triazole) bond previously studied via ab initio calculations.[9] The obtained lowest energy structure was then subjected to a 5 ns molecular dynamics simulation during which 500 structures were sampled. These 500 structures were subsequently minimised, and the local minimum structure obtained was used for further analysis. Models of the resulting modified duplexes are shown in Figures 5 and 6.

The DNA:RNA duplexes with four consecutive incorporations of either **X**,[9] **Y** and **Z** (Fig. 5) were found to be A/B-type duplexes with almost perfect stacking between both triazoles and phenyl moieties. However, some differences were observed. In the duplex with the phenol moieties **Y**, the aromatic rings seems to bend slightly away towards the 5′-end, perhaps from a repulsion between the hydroxy groups. The duplex with the sulfonamide monomer **Z**, on the other hand, demonstrated a perfect stacking of the aromatic rings and apparently a consistent organisation between the neighbouring sulfonamide groups. Furthermore, some distortion in the duplex inclination was observed in all three cases but most pronounced with **Z**. Thus, a short 2.8 Å distance consistent with hydrogen-bonding was observed between the second sulfonamide group from the 5′-end in **ON6-Z** and the 2′-hydroxyl group of the 5′-terminal cytosine in the complementary RNA strand. This seemed to be forcing the duplex to bend, although, the Watson–Crick base pairing was conserved.

Also the DNA:RNA duplexes with two consecutive incorporations of either **X**, **Y** and **Z** (Fig. 6) were found to be A/B-type duplexes. Stacking between the aromatic systems are observed in

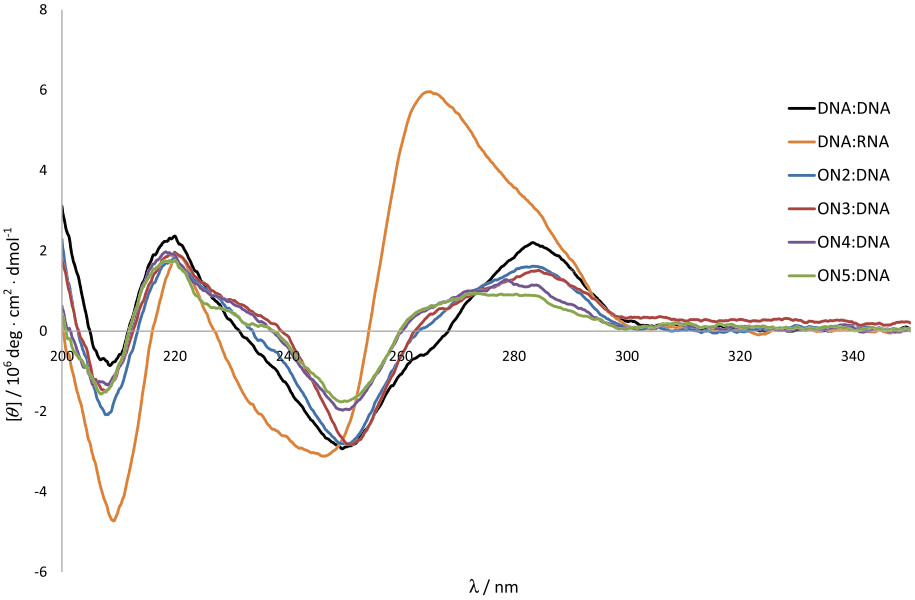

Figure 1. CD spectra of the DNA:DNA duplexes containing one to three incorporations of **X**.

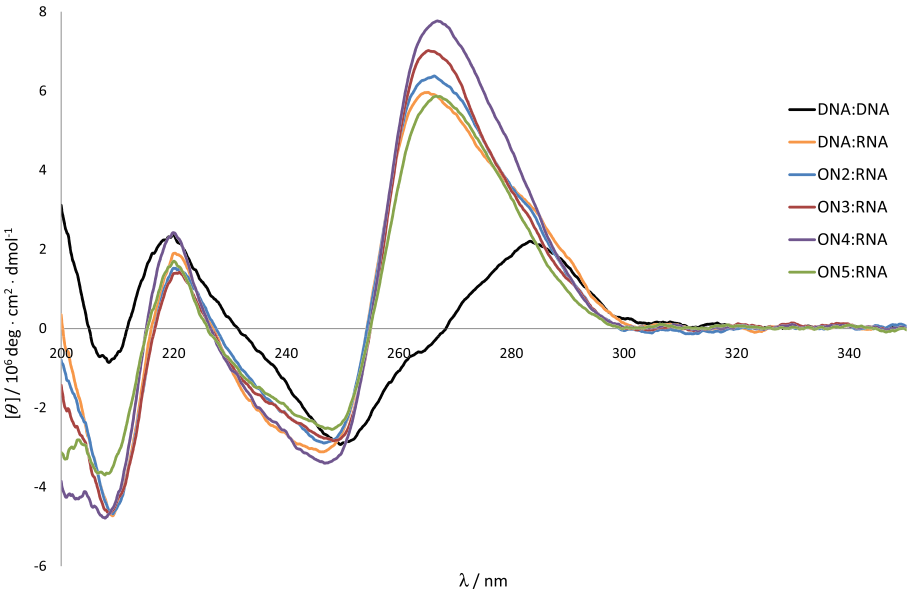

Figure 2. CD spectra of the DNA:RNA duplexes containing one to three incorporations of **X**.

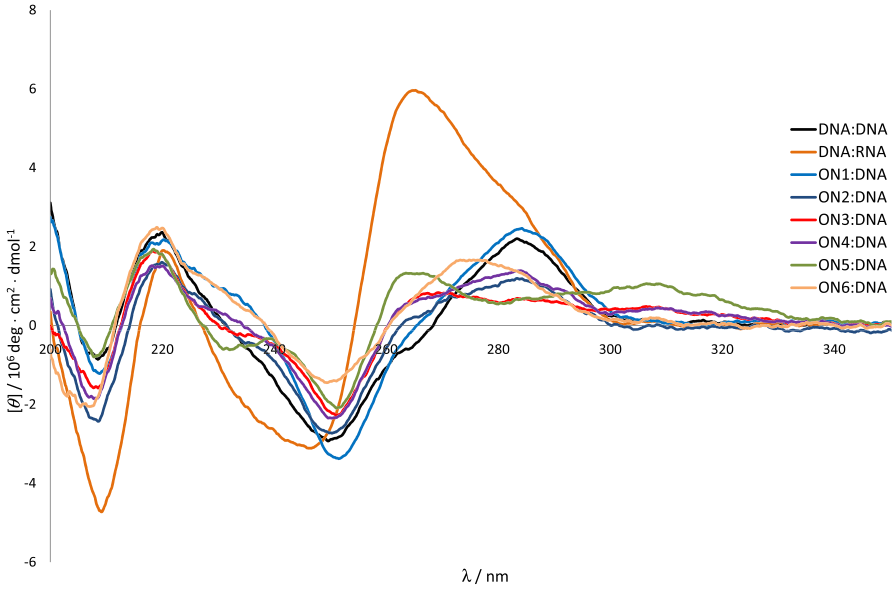

Figure 3. CD spectra of the DNA:DNA duplexes containing one to four incorporations of **Z**.

all three cases, although the two modified nucleobases were tilted out of the nucleobase plane pointing towards the 3′-end of the strand. This is less pronounced with the two monomers **X** but in the 3′-modification of the two, the co-planarity between the two heterocycles appeared to be lost. For monomer **Y**, this tilting of the modifications towards the 3′-end was even more pronounced, although no changes in the co-planarity were observed. An almost similar structure is seen with monomer **Z**.

3. Discussion

In the present study we have demonstrated the simple and efficient synthesis of two new nucleoside building blocks following the CuAAC method. Clearly, 5-ethynyl-2′-deoxyuridine, **1**, constitutes an obvious substrate for the easy preparation of various triazoles, and click chemistry is hereby a convenient method for introducing aromatic stacking in the major groove of nucleic acid duplexes.

The hybridisation data for the oligonucleotides of the current study followed the trend of our first study demonstrating that one incorporation of **X** lead to decreased stability of both DNA:DNA and DNA:RNA duplexes, whereas four consecutive incorporations of **X** demonstrate a net neutral effect on the stability of the DNA:DNA duplex and a massive increase in stability of the DNA:RNA duplex. Herein, we have demonstrated that the increase in duplex stability graduates by the number of modifications, and that two incorporations were enough to see the major part of the effect. The reason for the significant decrease in duplex stability obtained with single modifications with **X** might be found in the hydrophobicity of the phenyl group and the distortion in hydration of the duplex. This can, however, be

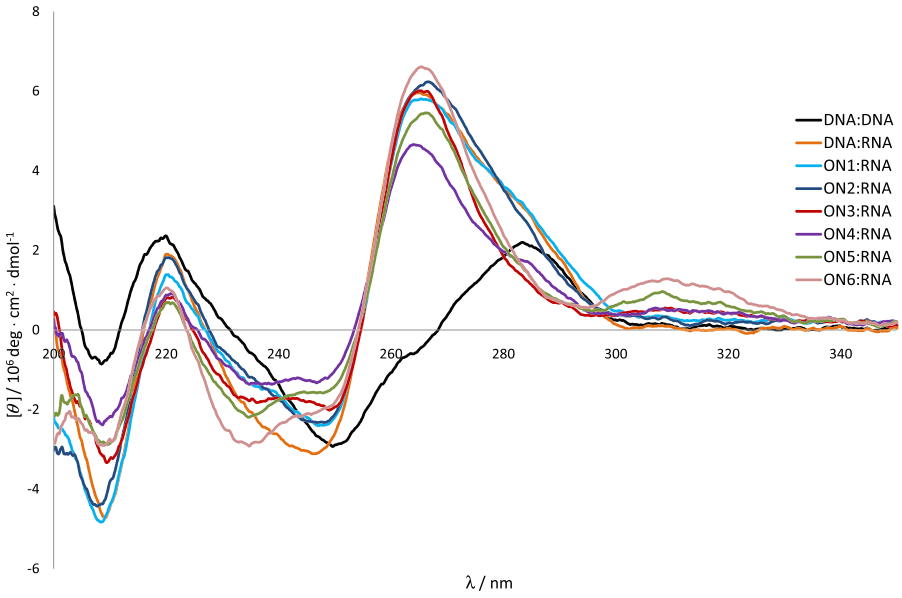

Figure 4. CD spectra of the DNA:RNA duplexes containing one to four incorporations of **Z**.

completely counterbalanced by the stacking of two phenyltriazole moieties as indicated by the very large increase in thermal stability of DNA:RNA duplexes when going from **ON1** and **ON2** to **ON3** and **ON4**. Also in the DNA:DNA duplexes some compensation by the second modification was clearly seen. The third and fourth consecutive incorporation of **X** lead to further relative increase in stabilisation up to an increase in thermal stability of the DNA:RNA duplex of 5 °C for each modification. The observation that only two consecutive incorporations of **X** were enough to give significant duplex stabilisation is very important for practical RNA-targeting, as the number of possible target sequences increases dramatically. Future studies will show, whether triazoles attached to other nucleobases can demonstrate the same duplex stabilisation by stacking with **X** hereby open the access to even more potential target RNA-sequences.

The two new derivatives **Y** and **Z** displayed almost similar influence on duplex stability as **X** indicating only small influence from the substituents on the distal phenyl position. In the DNA:DNA duplexes, the phenol **Y** seems to give the largest decreases in duplex stability, whereas the partial compensation obtained with consecutive incorporations seems to be most pronounced with the sulfonamide **Z**. In the DNA:RNA duplexes, the only obvious difference between **X**, **Y** and **Z** was that the stabilising effect of stacking three or four building blocks is even more pronounced with **Z** ending with the most stable duplex of the entire study with a T_m of 55.5 °C corresponding to a gain in thermal stability of +6.1 °C per modification.

When considering duplex structures as studied by modelling and CD-spectroscopy, some differences between the three modifications were indicated supporting the hybridisation data. The sulfonamide modification **Z** seems to have the largest impact on duplex structure of the three, probably due to the most efficient stacking behaviour. The modelling data indicated some bending of the DNA:RNA duplex with 4 × **Z** due to a hydrogen-bonding interaction across the major groove, and the CD-spectrum supported some deviation from the standard A/B-type duplex.

The current study demonstrated the value of π–π-stacking for obtaining duplexes with increased thermal stability. The effect of stacking was strongest in the DNA:RNA duplexes as compared to DNA:DNA duplexes, which might be due to the A/B-type duplex form being shorter and more compact than the B-type duplex. In the modified DNA:DNA, the increasing number of modifications and hereby the increasing stacking in the major groove was followed by a shift in duplex structure towards an A/B-type form as demonstrated by CD-spectroscopy. In the DNA:RNA duplex, the A/B-type was more or less retained when the modifications were introduced.

With the specific goal of targeting RNA, oligonucleotides containing enlarged bi- or tricyclic nucleobases or aromatic substituents on the nucleobases have been approached before.[4,6] In the case of the phenoxazine cytosine analogue, increased effect by the number of consecutive incorporations due to stacking in the major groove has also been demonstrated.[4] Nevertheless, the nucleoside monomers **X**, **Y** and **Z** from the current study demonstrates that this stacking effect can be obtained with simpler aromatic moieties obtained by straightforward click chemistry. This simple approach opens the possibility for a large variation of different entities in the major groove and with a much wider range of potential target sequences. The 5-(1,2,3-triazole-4-yl)pyrimidine nucleosides can therefore be important future building blocks for the development of antisense oligonucleotides.

4. Conclusions

From the easily available 5-ethynyl-2′-deoxyuridine, three simple nucleic acid building blocks introducing triazoles into the major groove of nucleic acid duplexes have been obtained. The stacking of triazoles, and the aromatic substituents attached, in the major groove leads to very stable DNA:RNA duplexes—the most stable containing a distal sulfonamide moiety. Efficient RNA-targeting, and hereby therapeutic potential, can be obtained with oligonucleotides containing only two consecutive incorporations of the triazoles.

5. Experimental section

All commercial reagents were used as supplied. Reactions were carried out under argon or nitrogen when anhydrous solvents were used. Column chromatography was performed with Silica Gel 60 (particle size 0.040–0.063 μm, Merck). NMR spectra

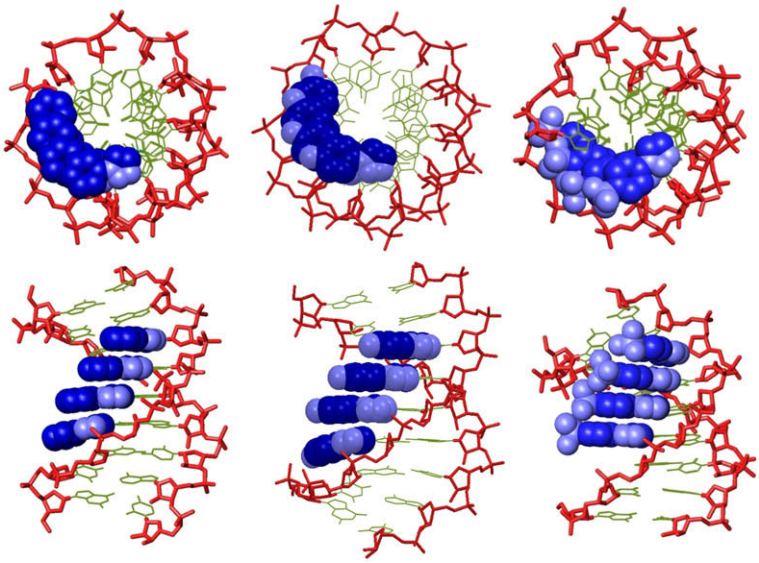

Figure 5. Modelling structures of modified DNA:RNA duplexes containing four consecutive incorporations of **X**, **Y** or **Z**. From left to right: **ON6**-**X**:RNA, **ON6**-**Y**:RNA, **ON6**-**Z**:RNA. Blue: 5-substituents with the heteroatoms in light blue; red: backbone; green: nucleobases.

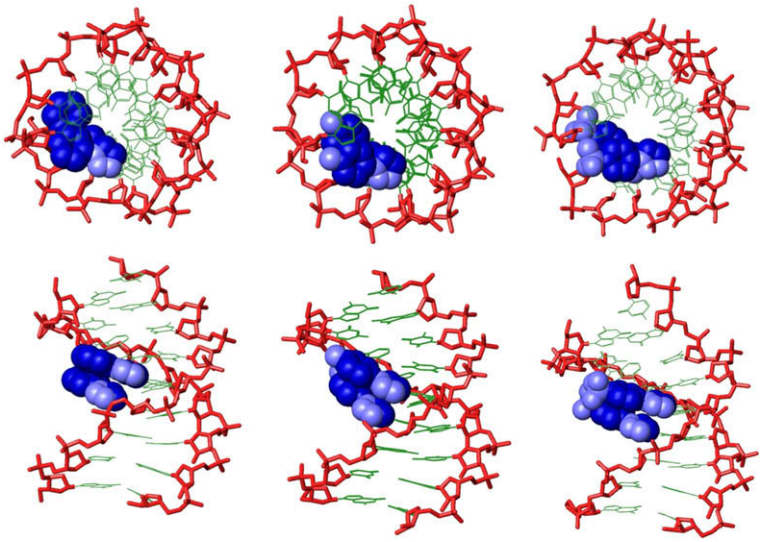

Figure 6. Modelling structures of modified DNA:RNA duplexes containing two consecutive incorporations of **X**, **Y** or **Z**. From left to right: **ON3**-**X**:RNA, **ON3**-**Y**:RNA, **ON3**-**Z**:RNA. Blue: 5-substituents with the heteroatoms in light blue; red: backbone; green: nucleobases.

were recorded on a Varian Gemini 2000 spectrometer or a Bruker Advance III 400 spectrometer. Values for δ are in ppm relative to tetramethylsilane as an internal standard or 85% H_3PO_4 as an external standard. Assignments of NMR-signals when given are based on 2D spectra and follow standard nucleoside convention. ESI mass spectra as well as accurate mass determinations were performed on a Thermo Finnigan TSQ 700 spectrometer. Microwave heated reactions were performed on an Emrys™ Creator.

5.1. Synthesis of 5-(1-(4-(*tert*-butyldimethylsilyloxy)phenyl)-1,2,3-triazol-4-yl)-5′-(4,4′-dimethoxytrityl)-2′-deoxyuridine (5)

To a solution of nucleoside **4** (485 mg, 0.88 mmol) and the azide **10** in ethanol and water (10 mL, 7:3, v/v) was added CuI (108 mg, 0.57 mmol), sodium ascorbate (281 mg, 1.42 mmol) and pyridine (3 mL). The mixture was stirred at rt for 4.5 h and then concentrated under reduced pressure. The residue was co-evaporated with toluene (2 × 10 mL), and methanol (10 mL), and then purified by column chromatography (0–10% CH_3OH in CH_2Cl_2) to give the nucleoside **5** (550 mg, 78%) as a white foam. R_f 0.3 (5% MeOH in CH_2Cl_2). ^{1}H NMR (DMSO-d_6; 300 MHz) δ 11.81 (s, 1H, NH), 8.72 (s, 1H, triazole-H), 8.40 (s, 1H, H-6), 7.77 (d, 2H, J = 8.9 Hz, Ar), 7.39 (m, 2H, Ar), 7.29–7.21 (m, 6H, Ar), 7.15 (m, 1H, Ar), 7.04 (d, 2H, J = 8.9 Hz, Ar), 6.82 (dd, 4H, J = 8.7, 1.5 Hz, Ar), 6.21 (t, 1H, J = 6.3 Hz, H-1′), 5.37 (d, 1H, J = 4.5 Hz, 3′-OH), 4.23 (m, 1H, H-3′), 3.98 (m, 1H, H-4′), 3.68 (s, 3H, OCH_3), 3.67 (s, 3H, OCH_3), 3.25–3.22 (m, 2H, H-5′), 2.33–2.27 (m, 2H, H-2′), 0.98 (s, 9H, $(CH_3)_3C$), 0.24 (s, 6H, $(CH_3)_2Si$). ^{13}C NMR (DMSO-d_6; 75 MHz) δ 161.1 (C-4), 158.0, 155.3 (Ar), 149.7 (C-2), 149.4, 144.8 (Ar), 136.2, 135.5, 135.4 (C-6, Ar), 130.7 (C-4 triazole), 129.7, 129.6, 127.7, 127.6, 126.5, 121.9, 120.8 (Ar), 120.1 (C-5 triazole), 113.1 (Ar), 104.8 (C-5), 85.7 (C-4′), 85.7 (Ar_3C), 85.3 (C-1′), 70.4 (C-3′), 63.6 (C-5′), 54.9 (OCH_3), 39.5 (C-2′), 25.5 ($(CH_3)_3C$), 17.9 ($(CH_3)_3C$), −4.6

($(CH_3)_2Si$). HiRes ESI MS *m/z* (M+Na) found/calcd 826.3213/826.3243.

5.2. Synthesis of 5-(1-(4-(*N*-((dimethylamino)methylidene)aminosulfonyl)phenyl)-1,2,3-triazol-4-yl)-5′-(4,4′-dimethoxytrityl)-2′-deoxyuridine (6)

To a suspension of the nucleoside **4** (300 mg, 0.54 mmol), the azide **12** (178 mg, 0.70 mmol), sodium ascorbate (65 mg, 0.32 mmol) and $CuSO_4{\cdot}5H_2O$ (25 mg, 0.1 mmol) in H_2O/*t*-BuOH (8 mL, 1:1, v/v) was added THF (1 mL) and pyridine (0.25 mL). The resulting clear solution was stirred at rt for 14 h, and then diluted with CH_2Cl_2 (50 mL) and brine (30 mL). The phases were separated, and the organic phase was washed with a saturated aqueous solution of $NaHCO_3$ (30 mL). The combined aqueous phase was extracted with EtOAc (2 × 30 mL), and the combined organic phase was dried (Na_2SO_4), and concentrated under reduced pressure. The residue was purified by column chromatography (0–8% MeOH in CH_2Cl_2) to afford the nucleoside **6** (220 mg, 87%) as a white foam. R_f 0.3 (5% *i*-PrOH in $CHCl_3$). ^1H NMR ($CDCl_3$, 400 MHz) δ 8.70 (br s, 1H, NH), 8.55 (br s, 1H, HC=N), 8.17 (s, 1H, triazole-H), 8.06 (m, 2H, Ar), 7.90 (d, 2H, *J* = 8.0 Hz, Ar), 7.40 (d, 2H, *J* = 7.6 Hz, Ar), 7.33–7.12 (m, 8H, Ar, H-6), 6.82 (m, 4H, Ar), 6.32 (t, 1H, *J* = 6.0 Hz, H-1′), 4.45 (br s, 1H, H-3′), 4.07 (m, 1H, H-4′), 3.74 (s, 6H, OCH_3), 3.45–3.29 (m, 2H, H-5′), 3.16 (s, 3H, CH_3), 3.05 (s, 3H, CH_3), 2.48 (m, 1H, H-2′), 2.31 (m, 1H, H-2′). ^{13}C NMR ($CDCl_3$, 100 MHz) δ 160.9, 158.58, 158.56, 144.6, 142.4, 135.7, 135.6, 130.1, 130.1, 128.3, 128.1, 127.9, 126.9, 120.2, 113.3, 86.9, 85.9, 77.2, 72.5, 63.6, 55.2, 41.6, 35.7. HiRes ESI MS *m/z* (M+Na) found/calcd 830.2610/830.2578.

5.3. Synthesis of 5-(1-(4-(*tert*-butyldimethylsilyloxy)phenyl)-1,2,3-triazol-4-yl)-5′-(4,4-dimethoxytrityl)-3′-*O*-(*P*-(2-cyanoethoxy)-*N*,*N*-diisopropylaminophosphinyl)-2′-deoxyuridine (7)

The nucleoside **5** (213 mg, 0.26 mmol) was dried by the coevaporation with anhydrous CH_2Cl_2 (2 × 5 mL) and dissolved in anhydrous CH_2Cl_2 (5.5 mL). DIPEA (0.23 mL, 1.33 mmol) and 2-cyanoethyl-*N*,*N*′-diisopropyl-phosphoramidochloridite (177 μL, 0.79 mmol) were added, and the mixture was stirred at rt for 1 h, 15 min. The solution was diluted with CH_2Cl_2 (25 mL) and washed with brine (25 mL) and water (25 mL). The organic phase was dried (Na_2SO_4) and concentrated under reduced pressure. The residue was purified by column chromatography (2–5% acetone in CH_2Cl_2) to give the product **7** (196 mg, 74%) as a white foam. R_f 0.8 (10% acetone in CH_2Cl_2). ^{31}P NMR (DMSO-d_6, 121.5 MHz) δ 148.6, 148.3. HiRes ESI MS *m/z* (M+Na) found/calcd 1026.4308/1026.4321).

5.4. Synthesis of 5-(1-(4-(*N*-((dimethylamino)methylidene)aminosulfonyl)phenyl)-1,2,3-triazol-4-yl)-5′-(4,4-dimethoxytrityl)-3′-*O*-(*P*-(2-cyanoethoxy)-*N*,*N*-diisopropylamino-phosphinyl)-2′-deoxyuridine (8)

The nucleoside **6** (300 mg, 0.37 mmol) was dried by the coevaporation with anhydrous CH_2Cl_2 (2 × 10 mL) and dissolved in anhydrous CH_2Cl_2 (10 mL). DIPEA (0.25 mL, 1.4 mmol) and 2-cyanoethyl-*N*,*N*′-diisopropyl-phosphoramidochloridite (0.25 mL, 1.1 mmol) were added, and the reaction mixture was stirred at rt for 4 h. The solution was diluted with CH_2Cl_2 (25 ml) and washed with a 5% aqueous solution of $NaHCO_3$ (2 × 10 mL). The aqueous phase was extracted with CH_2Cl_2 (2 × 10 mL) and the combined organic phase was dried (Na_2SO_4) and concentrated under reduced pressure. The residue was purified by column chromatography (0–96% EtOAc in petroleum ether) to give the phosphoramidite **8** (250 mg, 67%) as a white foam. R_f 0.5 (7.5% *i*-PrOH in $CHCl_3$). ^{31}P NMR ($CDCl_3$, 162 MHz) δ 149.1, 148.7. HiRes ESI MS *m/z* (M+Na) found/calcd 1030.3629/1030.3657.

5.5. Synthesis of *tert*-butyldimethylsilyl 4-azidophenylether (10)

A solution of the azide **9** (1.12 g, 8.27 mmol), *tert*-butyldimethylsilyl chloride (3.74 g, 24.8 mmol) and DMAP (0.5 g, 4.09 mmol) in a mixture of pyridine and acetonitrile (32 mL, 1:1, v/v) was stirred at rt for 48 h. The mixture was concentrated under reduced pressure and the residue was co-evaporated with toluene (2 × 20 mL) and methanol (10 mL). The residue was purified by column chromatography (CH_2Cl_2) to give the azide **10** (1.86 g, 90%) as a yellow liquid. R_f 0.9 (CH_2Cl_2). IR (KBr) 2122.4 cm^{-1}. ^1H NMR (DMSO-d_6, 300 MHz) δ 7.01 (m, 2H, Ar), 6.89 (m, 2H, Ar), 0.94 (s, 9H, $(CH_3)_3C$), 0.17 (s, 6H, $(CH_3)_2Si$). ^{13}C NMR (DMSO-d_6, 75 MHz) δ 152.5, 132.3, 121.2, 120.2 (Ar), 25.5 ($(CH_3)_3C$), 17.9 ($(CH_3)_3C$), −4.7 ($(CH_3)_2Si$). HiRes ESI MS *m/z* (M+Na) found/calcd 272.1184/272.1190.

5.6. Synthesis of *N*-dimethylaminomethylidene-4-azidobenzenesulfonamide (12)

To a cold stirred solution of $POCl_3$ (0.98 mL, 10.6 mmol) in dimethylformamide (20 mL) was added the azide **11** (1.05 g, 5.30 mmol). The reaction mixture was stirred at rt for 3 h, and then poured into cold water and neutralised with saturated aqueous ammonia. The formed precipitate was isolated, washed with water (100 mL) and dried to afford the product **12** (0.98 g, 73%) as white solid. R_f 0.4 (40% EtOAc in petroleum ether). Mp 155–156 °C. ^1H NMR (DMSO-d_6, 400 MHz) δ 8.21 (s, 1H, HC=N), 7.78 (d, 2H, *J* = 8.4 Hz, Ar), 7.24 (d, 2H, *J* = 8.4 Hz, Ar), 3.14 (s, 3H, CH_3), 2.90 (s, 3H, CH_3). ^{13}C NMR (DMSO-d_6, 100 MHz) δ 159.7, 142.8, 139.4, 127.8, 119.4 (Ar, C=N), 40.8, 35.0 (CH_3).

5.7. Synthesis of oligodeoxynucleotides

Oligonucleotide synthesis was carried out on an automated DNA synthesiser following the phosphoramidite approach. Synthesis of oligonucleotides **ON1–ON6** (**X–Z**) was performed on a 0.2 μmol scale by using the amidites **3**, **7** and **8** as well as the corresponding commercial 2-cyanoethyl phosphoramidites of the natural 2′-deoxynucleosides. The synthesis followed the regular protocol for the DNA synthesiser. For compound **3**, **7** and **8**, a prolonged coupling time of 20 min was used. 1*H*-Tetrazole was used as the activator and coupling yields for all 2-cyanoethyl phosphoramidites were 95–99.8%. The 5′-*O*-DMT-ON oligonucleotides were removed from the solid support by treatment with concentrated aqueous ammonia at 55 °C for 16 h, which also removed the protecting groups. The oligonucleotides were purified by reversed-phase HPLC on a Waters 600 system using a X_{terra} prep MS C_{18}; 10 μm; 7.8 × 150 mm column; buffer A: 0,05 M triethyl ammonium acetate pH 7.4. Buffer B: MeCN/H_2O (1:1). Program used: 2 min 100% A, 100–30% A over 38 min, 10 min 100% B, 10 min 100% A. All oligonucleotides were detritylated by treatment with an 80% aqueous solution of acetic acid for 20 min, quenched with a aqueous solution of sodium acetate (3 M, 15 μL) and then added sodium perchlorate (5 M, 15 μL) followed by acetone (1 mL). The pure oligonucleotides precipitated overnight at −20 °C. After centrifugation 12,000 rpm, 10 min at 4 °C, the supernatant was removed and the pellet washed with cold acetone (2 × 1 mL) and dried for 30 min under reduced pressure, and dissolved in pure water (500 μL). The concentration was determined by UV at 260 nm, and the purity confirmed by IC analysis. MALDI-TOF-MS $[M-H]^-$ gave the following results (calcd/found): **ON2-X** (2864.9/

2865.4); **ON3-X** (2994.0/2992.0); **ON4-X** (2994.0/ 2995.3); **ON5-X** (3124.5/3123.9); **ON1-Y** (2880.9/2878.0); **ON2-Y** (2881.3/2876.5); **ON3-Y** (3026.9/3024.7); **ON4-Y** (3026.0/3024.1); **ON5-Y** (3173.0/ 3171.7); **ON6-Y** (3316.0/ 3315.8); **ON1-Z** (2943.0/2941.8); **ON2-Z** (2943.0/2943.5); **ON3-Z** (3151.0/3146.0); **ON4-Z** (3151.0/)3147.0; **ON5-Z** (3526.8/3522.4); **ON6-Z** (3567.0/3567.0).

5.8. Thermal denaturation experiments

Extinction coefficients of the modified oligonucleotides were estimated from a standard method but calibrated by the micromolar extinction coefficients of the monomeric compounds **X**, **Y** and dT, which were estimated from their UV-spectra (dT: $\varepsilon_{260} = 8.5$, **X**: $\varepsilon_{260} = 7.8$, **Y**: $\varepsilon_{260} = 12.6$), and **Z**, which was estimated by ab initio calculated oscillator strength to be $\varepsilon_{260} \sim 8.0$; practically we used a $\varepsilon_{260} \sim 5.0$. UV melting experiments were thereafter carried out on a UV spectrometer. Samples were dissolved in a medium salt buffer containing 2.5 mM Na_2HPO_4, 5 mM NaH_2PO_4, 100 mM NaCl, and 0.1 mM EDTA at pH 7.0 with 1.5 μM concentrations of the two complementary sequences. The increase in absorbance at 260 nm as a function of time was recorded while the temperature was increased linearly from 5 to 60 or 75 °C at a rate of 0.5 or 1.0 °C/min by means of a Peltier temperature programmer. The melting temperature was determined as the local maximum of the first derivatives of the absorbance versus temperature curve. The melting curves were found to be reversible. All determinations are averages of at least duplicates within ±0.5 °C.

5.9. Circular dichroism spectroscopy

CD-spectra were obtained at 5 °C using the same medium salt buffer as in the UV melting experiments with 1.5 μM concentrations of the two complementary sequences.

5.10. Molecular modelling

The duplexes investigated (**ON3-X–Z** and **ON6-X–Z**) were built with a standard B-type helical geometry within the MACROMODEL V9.1 suite of programs.[14] In all the calculations the phosphodiester backbone charge was neutralised with sodium ions, placed 3.0 Å from the negatively charged oxygen atoms in the plane described by the phosphorus and the non-bridging oxygen atoms. The sodium–oxygen distances were restrained to 3.0 Å by a force constant of 418 kJ/mol Å^2. The modifications **X**, **Y** and **Z** were each subjected to a Monte Carlo conformational search[15] rotating the C5 (nucleobase)—C4 (triazole) bond and the N1 (triazole)—C1 (phenyl) bond to generate 1000 structures, which were minimised to identify the lowest energy structure. The lowest energy structure obtained from the Monte Carlo search was hereafter subjected to a 5 ns molecular dynamics simulation (simulation temperature 300 K, time step 2.2 fs, SHAKE all bonds to hydrogen), during which 500 structures were sampled and subsequently minimised. The duplex structures were minimised using the Polak–Ribiere Conjugate Gradient Method, the all-atom AMBER force field[16,17] and GB/SA solvation model[18] as implemented in MACROMODEL V9.1. Nonbonded interactions were treated with extended cut-offs (van der Waals 8.0 Å and electrostatics 20.0 Å). Oscillator strength calculations for monomer **Z** were performed using a Hartree–Fock water model with the aug-pc-1 basis set in GAUSSIAN 3.[19]

Acknowledgements

The project was supported by The Danish Research Agency's Programme for Young Researchers, Nucleic Acid Center and The Danish National Research Foundation, The Nucleic Acid Based Drug Design Training Center (NAC-DRUG) in the Sixth Framework Programme Marie Curie Host Fellowships for Early Stage Research Training under contract no. MEST-CT-2004-504018, The Danish Natural Science Research Council, Danish Center for Scientific Computing and Møllerens Fond. Mrs. Birthe Haack and Mr. Christian Schneider are thanked for technical assistance.

References and notes

1. (a) Yan, H. *Science* **2004**, *306*, 2048; (b) Wengel, J. *Org. Biomol. Chem.* **2004**, *2*, 277.
2. Kurreck, J. *Eur. J. Biochem.* **2003**, *270*, 1628.
3. Luyten, I.; Herdewijn, P. *Eur. J. Med. Chem.* **1998**, *33*, 515.
4. Lin, K.-Y.; Jones, R. J.; Matteucci, M. *J. Am. Chem. Soc.* **1995**, *117*, 3873.
5. Wagner, R. W.; Matteucci, M. D.; Lewis, J. G.; Gutierrez, A. J.; Moulds, C. M.; Froehler, B. C. *Science* **1993**, *260*, 1510.
6. (a) Gutierrez, A. J.; Matteucci, M. D.; Grant, D.; Matsumura, S.; Wagner, R. W.; Froehler, B. C. *Biochemistry* **1997**, *36*, 743; (b) Gutierrez, A. J.; Terhorst, T. J.; Matteucci, M. D.; Froehler, B. C. *J. Am. Chem. Soc.* **1994**, *116*, 5540; (c) Sinkeldam, R. W.; Greco, N. J.; Tor, Y. *ChemBioChem* **2008**, *9*, 706.
7. (a) Kolb, H. C.; Finn, M. G.; Sharpless, K. B. *Angew. Chem., Int. Ed.* **2001**, *40*, 2004; (b) Kolb, H. C.; Sharpless, K. B. *Drug Discovery Today* **2003**, *8*, 1128.
8. (a) Tornøe, C. W.; Christensen, C.; Meldal, M. *J. Org. Chem.* **2002**, *67*, 3057; (b) Rostovtsev, V. V.; Green, L. G.; Fokin, V. V.; Sharpless, K. B. *Angew. Chem., Int. Ed.* **2002**, *41*, 2596.
9. Kočalka, P.; Andersen, N. K.; Jensen, F.; Nielsen, P. *ChemBioChem* **2007**, *8*, 2106.
10. (a) Burley, G. A.; Gierlich, J.; Mofid, M. R.; Nir, H.; Tal, S.; Eichen, Y.; Carell, T. *J. Am. Chem. Soc.* **2006**, *128*, 1398; (b) Gierlich, J.; Burley, G. A.; Gramlich, P. M. E.; Hammond, D. M.; Carell, T. *Org. Lett.* **2006**, *8*, 3639.
11. Buck, S. B.; Bradford, J.; Gee, K. R.; Agnew, B. J.; Clarke, S. T.; Salic, A. *BioTechniques* **2008**, *44*, 927.
12. (a) Andersen, J.; Madsen, U.; Björkling, F.; Liang, X. *Synlett* **2005**, 2209; (b) Cai, Q.; Zhu, W.; Zhang, H.; Zhang, Y.; Ma, D. *Synthesis* **2005**, 496.
13. Wilkinson, B. L.; Bornaghi, L. F.; Houston, T. A.; Innocenti, A.; Wullo, D.; Supuran, C. T.; Poulsen, S. A. *J. Med. Chem.* **2007**, *50*, 1651.
14. MACROMODEL, Version 9.1, Schrödinger, LLC, New York, NY, 2005.
15. Chang, G.; Guida, W. C.; Still, W. C. *J. Am. Chem. Soc.* **1989**, *111*, 4379.
16. Weiner, S. J.; Kollman, P. A.; Case, D. A.; Singh, U. C.; Ghio, C.; Alagona, G.; Profeta, S.; Weiner, P. *J. Am. Chem. Soc.* **1984**, *106*, 765.
17. Weiner, S. J.; Kollman, P. A.; Nguyen, D. T.; Case, D. A. *J. Comput. Chem.* **1986**, *7*, 230.
18. Still, W. C.; Tempcyk, A.; Hawley, R. C.; Hendrickson, T. *J. Am. Chem. Soc.* **1990**, *112*, 6127.
19. GAUSSIAN-03. Gaussian Inc., 340 Quinnipiac St., Bldg 40, Wallingford, CT 06492, USA.